

## Designing Machine Learning-Optimized Nitrogen and Sulfur Co-doped CoNi@SiO<sub>2</sub> Electrocatalyst for High Performance Oxygen Evolution Reaction

Mohammad Waseem<sup>a</sup>, Salah M. El-Bahy<sup>b</sup>, Mehar Muhammad Hamza Maqbool<sup>a</sup>, Noor ul Islam<sup>c</sup> Farhan Zafar<sup>d</sup>,  
Muhammad Ali Khan<sup>a\*</sup>, Naeem Akhtar<sup>a\*</sup>, Muhammad Sohail<sup>a</sup>, Mujahid Abbas<sup>a</sup>, Adel Qlayet Alkhedaide<sup>e</sup>, Cong Yu<sup>f\*</sup>

<sup>a</sup>Institute of Chemical Sciences, Bahauddin Zakariya University (BZU), Multan 60800, Pakistan

<sup>b</sup>Department of Chemistry, Turabah University College, Taif University, P.O. Box 11099, Taif 21944, Saudi Arabia

<sup>c</sup>Faculty of Law, Management and social sciences, University of Bradford, Bradford, United Kingdom

<sup>d</sup>Department of Chemistry, COMSATS University Islamabad, Lahore Campus, Lahore 54000, Pakistan

<sup>e</sup>Department of Clinical Laboratory Sciences, Turabah University College, Taif University, P.O. Box 11099, Taif 21944, Saudi Arabia

<sup>f</sup>State Key Laboratory of Electroanalytical Chemistry, Changchun Institute of Applied Chemistry, Chinese Academy of Sciences, Changchun 130022, China

### Corresponding Author

\*Naeem Akhtar [naeemakhtar@bzu.edu.pk](mailto:naeemakhtar@bzu.edu.pk)

\*Muhammad Ali Khan [malikhan@bzu.edu.pk](mailto:malikhan@bzu.edu.pk)

## **S1. Instrument details**

Instruments used during this scientific work were Fourier transform infrared spectroscopy (FTIR) IRA affinity-1S spectrophotometer-USA to record FTIR spectra in the range of 500-4000  $\text{cm}^{-1}$ . X-ray diffraction (XRD) diffractograms were measured by Rigaku, Miniflex-II-Japan by means of  $\text{Cu K}\alpha$  (with a scan angle:  $5-80^\circ$ , at 40 kV, and 40 mA). The surface morphology was analyzed using MAIA3 TESCAN Scanning Electron Microscope (SEM) and ZEISS Gemini. A JEOL JEM-1400 transmission electron microscopy (TEM) instrument with an accelerating voltage of 100 kV was used. Brunauer–Emmett–Teller (BET) surface area was studied through Tristar II 3020. All the electrochemical investigations were carried out using the Gamry interface (1010E) potentiostat. This potentiostat instrument contains three electrodes such as working electrode, reference electrode and auxiliary electrode. In this work, synthesized electrodes were used as working electrode,  $\text{Ag}/\text{AgCl}$  used as reference electrode and platinum wire used as auxiliary electrode.

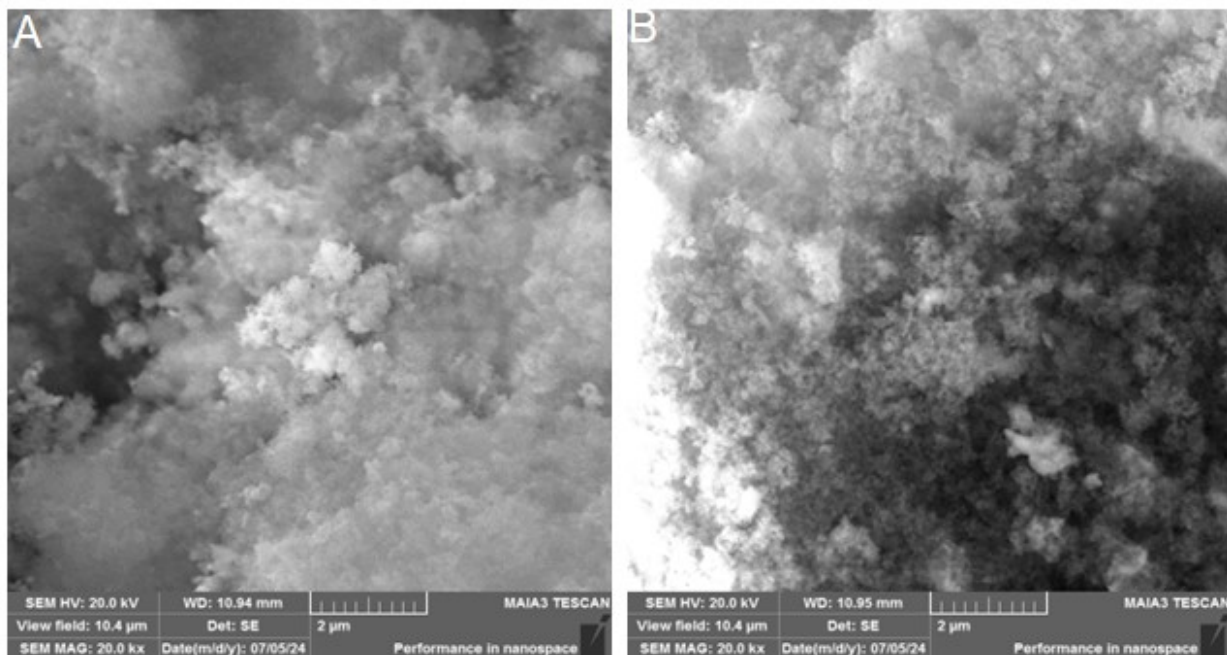
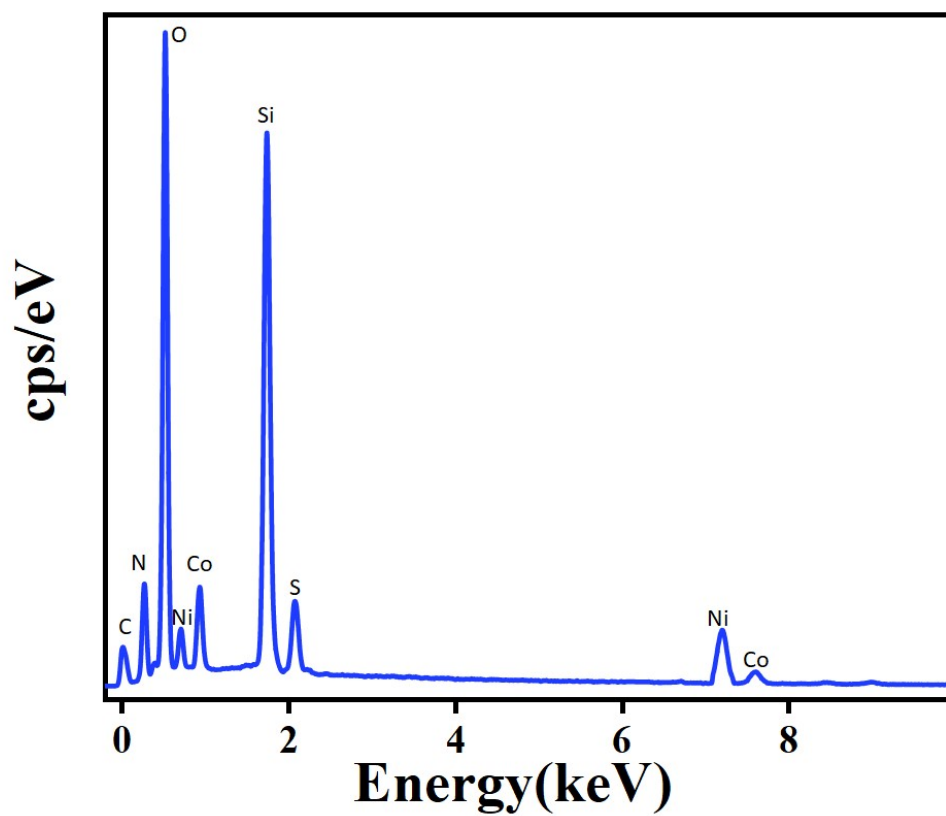
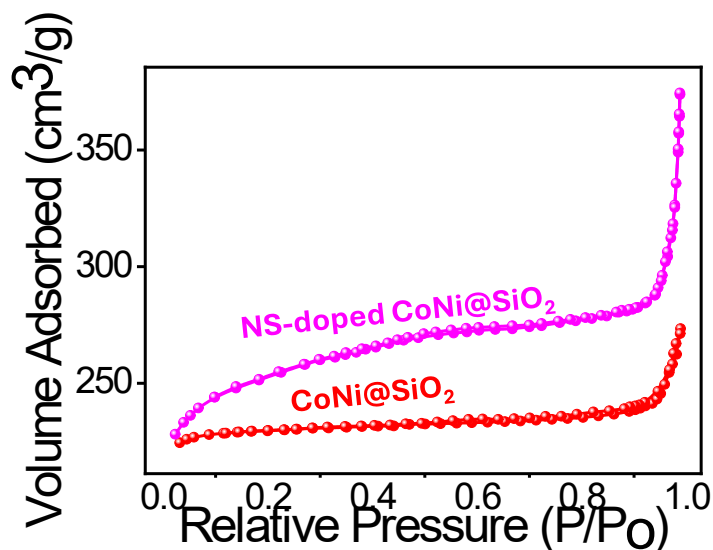


Figure S1. SEM images of (A) CoNi@SiO<sub>2</sub>, (B) NS-doped CoNi@SiO<sub>2</sub>.



**Figure S2.** Shows the EDX spectrum of NS-doped CoNi@SiO<sub>2</sub>.



**Figure S3.** Shows the BET spectrum of CoNi@SiO<sub>2</sub> and NS-doped CoNi@SiO<sub>2</sub>.

## S2. Machine Learning for Optimization and Evaluation

The present study delved into examining the impact of ML in predicting overpotential on various compositions of fabricated materials involving implementation of various regression models (linear regression (LR), ridge regression (RR), decision tree regression (DTR), random forest regression (RFR), gradient boosting regression (GBR), K-nearest neighbors' regression (KNNR), support vector regression (SVR), and extreme gradient boosting regression (XGBR)) on experimental dataset. Multiple regression models, were employed to establish quantitative relationship between a dependent variable (Overpotential) and one or more independent variables (concentration of Ni(NO<sub>3</sub>)<sub>2</sub>·6H<sub>2</sub>O Co(NO<sub>3</sub>)<sub>2</sub>·6H<sub>2</sub>O and thiourea). The evaluation of dataset done by regression model primarily centers on the partitioning of available data into three distinct subsets: the training set, the validation set, and the test/prediction set. Initially, the training dataset is employed to train the regression models, followed by rigorous testing against both the validation and test datasets. The evaluation of a multiple regression model primarily centres on the partitioning of available data into three distinct subsets: the training set, the validation set, and the test/prediction set. Initially, the training dataset is employed to simulate

the multiple regression models, followed by rigorous testing against both the validation and test datasets utilizing Python. The performance and accuracy of predictions are meticulously analysed through the error metrics, specifically Mean Squared Error (MSE) and R-squared ( $R^2$ ).

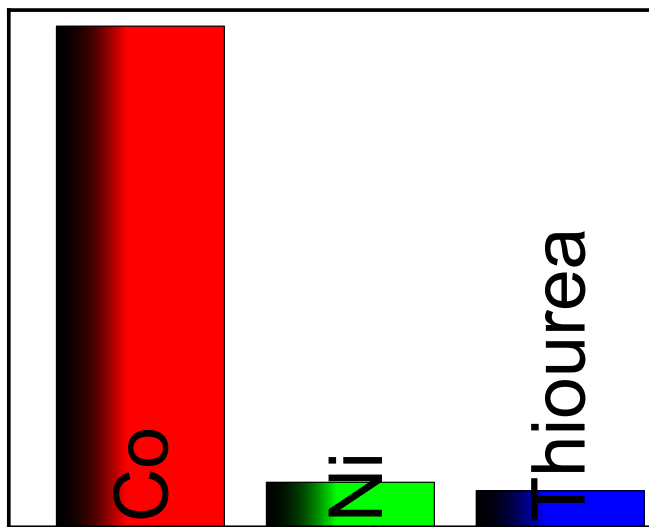


**Figure S4.** shows the importance feature graph

### S3. Electrochemical measurement

A computer-controlled GAMRY Potentiostat workstation was employed for all electrochemical studies, including cyclic voltammetry (CV), linear sweep voltammetry (LSV), electrochemical impedance spectroscopy (EIS), and chronoamperometry to investigate water oxidation. CV was utilized to examine the redox processes occurring at the electrode/electrolyte interface, while electrochemical impedance spectroscopy was used to measure the electrical resistance of specific analytes.

The electrochemical experiments were conducted using a standard three-electrode system housed in a glass cell. To clean the electrochemical cell, it was initially washed with a 3:1 mixture

of HNO<sub>3</sub> and H<sub>2</sub>SO<sub>4</sub>, followed by rinsing with ultrapure distilled water. The cell was then rinsed multiple times with ultrapure distilled water and acetone, and subsequently dried in an oven at 80°C for 30-40 minutes. Prior to placing the counter electrode (Pt wire) into the electrochemical cell, it was washed with ultrapure water and dipped in a 20% HNO<sub>3</sub> solution for a few minutes. All measurements were performed at room temperature in a 1 M KOH electrolyte solution with a pH of 13.5. CV was performed by cycling the potential from positive to negative at scan rates of 5 to 25 mV s<sup>-1</sup>. The electrolyte solution was purged with argon gas for 30 minutes before measuring electrochemical activity. All current values were calculated based on the geometrical area of the working electrode. All potentials were recorded after 50 percent IR adjustment, which was done manually using the formula:

$$E_{actual} = E_{experimental} - IR \quad (S1)$$

The following equation was used to convert all potential collected vs. Ag/AgCl into RHE potential:

$$E_{RHE} = E_{Ag/AgCl} + 0.059 \text{ pH} + E_0_{Ag/AgCl} \quad (S2)$$

In this context,  $E_{Ag/AgCl}$  represents the measured potential against the Ag/AgCl electrode,  $E_0_{Ag/AgCl}$  represents the typical thermodynamic potential (0.197 V) of Ag/AgCl, and  $E_{RHE}$  represents the estimated potential vs. RHE.

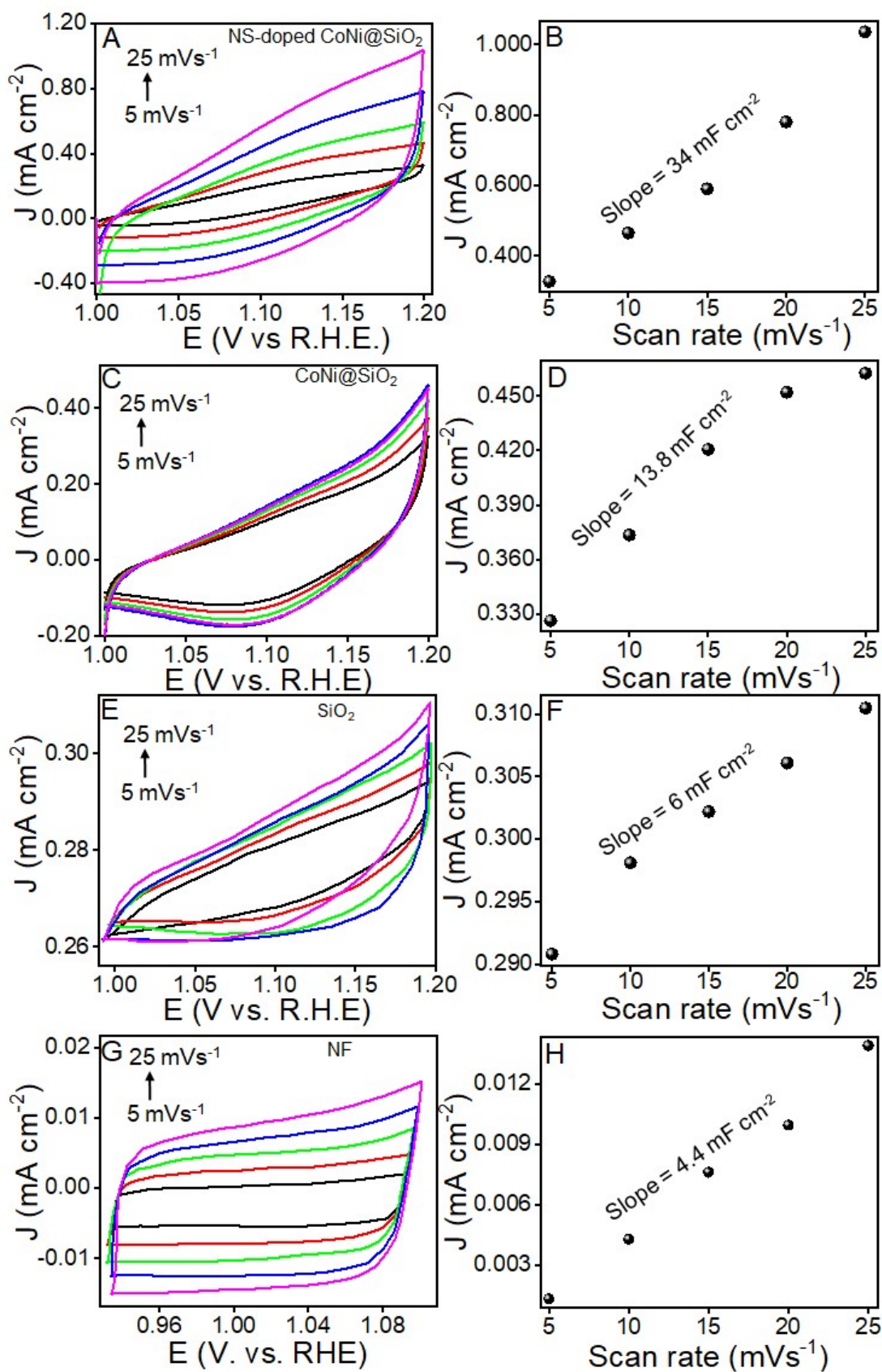


**Figure S5.** Evaluation of electrocatalytic activity through CV in non-faradaic region (A, C, E, G) of NS-doped CoNi@SiO<sub>2</sub>, CoNi@SiO<sub>2</sub>, SiO<sub>2</sub> and NF electrodes respectively & (B, D, F & H) represent the graphs plotted between current density and scan rate (5-25 mVs<sup>-1</sup>) of NS-doped CoNi@SiO<sub>2</sub>, CoNi@SiO<sub>2</sub>, SiO<sub>2</sub> and NF.

### **S3.1 Tafel Slope calculations from the polarization curve of NS-doped CoNi@SiO<sub>2</sub>, CoNi@SiO<sub>2</sub>, SiO<sub>2</sub>, and NF**

To evaluate the kinetics and catalytic performance, Tafel plot was plotted between over potential and log of current density in the linear portion of steady state polarization curve. It can be described using the equation.

$$\eta = a + \left(2.303 \frac{RT}{\alpha n F}\right) * \log j \quad (S3)$$

Here, over potential is represented by  $\eta$ , charge transfer coefficient by  $\alpha$ , the number of electrons take part in reaction by  $n$ , current density by  $j$ , faraday constant by  $F$ . The  $2.303RT/\alpha nF$  value refers to the slope.

### **S3.2 Electrochemically active surface area of NS-doped CoNi@SiO<sub>2</sub>, CoNi@SiO<sub>2</sub>, SiO<sub>2</sub>, and NF**

Evaluating the electrochemical double-layer capacitance and performing CV measurements at various scans ranging from 5-25 mV/s, the electrochemically active surface area of the catalyst was measured. By fitting the average current density vs scan rate curve, the electrochemical capacitance may be calculated easily. The CV was performed within a non-faradic region. The electrochemical active area was calculated by adopting already reported method [S<sup>1</sup>] and is given below

$$C_{dl} = slope * 1000 / 2 \quad (S4)$$

$$C_{dl} \text{ of NS-doped CoNi@SiO}_2 = slope * 1000 / 2 = 0.00762 * 1000 / 2 = 3.81 \text{ mF cm}^{-2}$$

$$C_{dl} \text{ of CoNi@SiO}_2 = \text{slope} * 1000 / 2 = 0.00508 * 1000 / 2 = 2.54 \text{ mF cm}^{-2}$$

$$C_{dl} \text{ of SiO}_2 = \text{slope} * 1000 / 2 = 0.000676 * 1000 / 2 = 0.338 \text{ mF cm}^{-2}$$

$$C_{dl} \text{ of NF} = \text{slope} * 1000 / 2 = 0.000448 * 1000 / 2 = 0.224 \text{ mF cm}^{-2}$$

$$\text{Electro-active surface area} = C_{dl} / C_{sp} \text{ (S5)}$$

$$\text{Electro-active surface area of NS-doped CoNi@SiO}_2 = 3.81 / 0.04 = 95.25 \text{ cm}^2$$

$$\text{Electro-active surface area of CoNi@SiO}_2 = 2.54 / 0.04 = 63.5 \text{ cm}^2$$

$$\text{Electro-active surface area of SiO}_2 = 0.338 / 0.04 = 8.45 \text{ cm}^2$$

$$\text{Electro-active surface area of NF} = 0.224 / 0.04 = 5.6 \text{ cm}^2$$

### S3.3 OH<sup>-</sup> ion adsorption capability of the developed electrodes

Laviron equation is given below

$$E_c = E_{1/2} - \left( \frac{RT}{\alpha n F} \right) * \ln \left( \frac{\alpha n F}{RT k_s} \right) - \left( \frac{RT}{\alpha n F} \right) * \ln (v) \text{ (S6)}$$

Where  $E_c$  and  $E_{1/2}$  are the reduction and formal potential of metal redox T, F,  $k_s$  and R, stand for absolute temperature, Faraday constant, redox constant, and general gas constant, respectively. Whereas n and  $\alpha$  represent the number of electrons transferred and electron transfer coefficient.

**Table S1. represents the RMSE, and %R<sup>2</sup> of each ML algorithm on training, validation, and test dataset**

Model	Train RMSE	Validation RMSE	Test RMSE	R <sup>2</sup> Score
Linear Regression	4.75	4.76	4.70	0.81
Ridge Regression	4.75	4.76	4.70	0.81
Decision Tree Regression	0.00	2.95	2.79	0.93
Random Forest Regression	1.45	2.77	3.24	0.91
Gradient Boosting Regression	0.54	2.03	2.04	0.96
K-nearest neighbor Regression	3.36	5.98	4.26	0.85

Support Vector Regression	6.58	9.23	8.08	0.44
XGBoost Regression	0.00	2.47	2.20	0.96

**Table S2. Comparison table of Tafel slope with already reported electrode**

Sr. No	Electrode	Tafel Slope (mV/dec)	Overpotential at 10 mA cm <sup>-2</sup> (mV)	Reference
1	Co <sub>3</sub> O <sub>4</sub> /MgO–SiO <sub>2</sub>	88	340	S <sup>2</sup>
2	SV-CoSiO <sub>2</sub>	88	301	S <sup>3</sup>
3	SiO <sub>2</sub> /Co <sub>x</sub> P	120	293	S <sup>4</sup>
4	Fe <sub>3</sub> O <sub>4</sub> @SiO <sub>2</sub> @NiO/graphene/C <sub>3</sub> N <sub>4</sub>	40.46	288	S <sup>5</sup>
5	ZnO-Co <sub>3</sub> O <sub>4</sub> /C	44.5	270	S <sup>6</sup>
6	Mo/CoFe LDH	59	266	S <sup>7</sup>
7	SiO <sub>2</sub> @TiN/NF	40	256	S <sup>8</sup>
8	rGO/ZnSnO <sub>3</sub>	37	212	S <sup>9</sup>
9	NS-doped CoNi@SiO <sub>2</sub>	103.9	200	This work

**Reference:**

1. S. Manzoor, A. G. Abid, F. Hussain, A. Shah, R. A. Pashameah, E. Alzahrani, S. M. El-Bahy, T. Taha and M. N. J. F. Ashiq, 2022, **328**, 125264.
2. G. Ali, A. Tahira, A. Hayat, M. A. Bhatti, A. A. Shah, S. N. U. S. Bukhari, E. Dawi, A. Nafady, R. H. Alshammari and M. Tonezzer, *RSC advances*, 2024, **14**, 38009-38021.
3. Y. Wang, L. Li, S. Wang, X. Dong, C. Ding, Y. Mu, M. Cui, T. Hu, C. Meng and Y. Zhang, *Small*, 2024, **20**, 2401394.
4. X. Zeng, H. Zhang, X. Zhang, Q. Zhang, Y. Chen, R. Yu and M. Moskovits, *Nano Materials Science*, 2022, **4**, 393-399.
5. L. Ye, P. Zhu, T. Wang, X. Li and L. Zhuang, *Nanoscale Advances*, 2023, **5**, 4852-4862.
6. F. Zafar, M. Asad, W. Sajjad, M. A. Khan, N. Akhtar, S. U. Hassan and C. Yu, *International Journal of Hydrogen Energy*, 2025, **98**, 384-393.
7. C. Y. J. Lim, R. I. Made, Z. H. J. Khoo, C. K. Ng, Y. Bai, J. Wang, G. Yang, A. D. Handoko and Y.-F. Lim, *Materials Horizons*, 2023, **10**, 5022-5031.
8. A. A. Alothman, S. I. A. Shah, A. G. Abid, M. U. Nisa, N. Bibi, K. Jabbour, M. I. Anwar, M. F. Ehsan and S. Manzoor, *ChemistrySelect*, 2024, **9**, e202303619.
9. F. F. Alharbi, S. M. Gouadria, L. Alhawali, S. Aman and H. M. T. Farid, *Diamond and Related Materials*, 2024, **148**, 111456.